The Power Consumption of Paddlewheel Aerator with Moveable Blades

Samsul Bahri[1,*], Radite Praeko Agus Setiawan[2], Wawan Hermawan[2] and Muhammad Zairin Junior[3]

[1,*]Department of Mechanical Engineering, Lhokseumawe State Polytechnic
Buketrata, Lhokseumawe 24301, Indonesia
[2]Department of Mechanical and Biosystem Engineering, Bogor Agricultural University
Dramaga, Bogor 16680, Indonesia
[3]Departmentof Aquaculture, Bogor Agricultural University, Dramaga, Bogor 16680, Indonesia
*Corresponding Author: samsul@pnl.ac.id

Abstract

The development movable blade of paddlewheel aerator is considered on fact that power is required when the blade of paddle wheel aerator entering water and contrary action of aeration effect while the blade is leaving the water. This study was carried out to design and simulate paddlewheel aerator with movable blade which will open when entering water and close when leaving water. The blade is closed at quadrant I and IV (entering water surface) and open at quadrant III and II (leaving water surface). The design of the blade was refered to commonly used as Taiwan wheel type. The component of movable blade mechanism consisted of cam, shaft, rim, rim cap, blade holder, follower, spring and bearing. The follower was able to rotate with angle of rotation of 125˚, the rotational displacement of 50 mm, the maximum velocity of 0.55 m/s and the acceleration of 6.09 m/s^2. The result shows that the testing without a load at 115 rpm, the torque that occuredis 43.05 N·m and the electric power consumption is 511.72 Watt. However, the electrical consumption is still higher comparing with Taiwan aerator model due to the friction occured on the follower and cam.

Keywords:Paddlewheel aerator, movable blade, cam–follower mechanism, torque, power

Introduction

Aeration is a mechanism of adding some amount of oxygen into water to provide sufficient amount of oxygen. Aeration is carried out by increasing water and air contact using aerator device. One type of aerator device which widely used in pond farming is paddle wheel aerator (Laksitanonta, 2003). Paddle wheel aerator is considered as the most appropriate aerator device due to aeration mechanism and wide usable driven power (Romaire and Merry, 2007).

Some of parameters including water and air surface contact, differential oxygen concentration, film surface coefficient and turbulence influence aeration rate (Boyd 1998). Aeration performance was influenced by geometry, size and wheel velocity (Moulick, *etal*., 2002). Higher size tends to have higher aeration which simultaneously followed by higher driven power needs due to higher drag force. This condition creates certain problem in utilizing paddle wheel aerator as it may increase operational cost including electrical and fuel consumption.

Various models of paddle wheel aerator are offered in market. Aerator made by Taiwan is widely used by consumers due to affordable price, light in weight and corrosion–resistant but has low efficiency (Wyban, 1989). Aerator that was designed and fabricated by Taiwan has *SAE* (standard aeration efficiency) value of 1.063 kg O_2 kW h^{-1} (Peterson & Walker 2002). Bhuyar, *et al.*, (2009) designed aerator with SAE value 2.269 kg O_2 kWh^{-1}. The most appropriate paddle wheel aerator was designed by Moore and Boyd with *SAE* value 2.54 kg O_2 kWh^{-1}. Some of fabrications use aerator design with specification 2.25–7.5 kW and *SOTR* 17.4–23.2 kg O_2 h^{-1} and average value of SAE was 2.2 kg O_2 kW h^{-1} (Moore & Boyd 1992).

Up to now, the development of paddle wheel aerator still uses non–movable blade which result in less optimum power consumption because power is linear with the increasing of aeration rate. Therefore, development of movable blade is needed due to aeration power is only required when blade entering water and in contrary the aeration effect only occurs when blade is about to leaving the water. Therefore movable blade was designed to open when leaving water and close when entering water. This study was aimed to design and simulate paddle wheel aerator with movable blade to reduce drag force acting on blade as well as power consumption.

Functional Design and Testing Methods

Functional Design

The wheel was designed to rotate clockwise with movable blade that enabled to open and close. The blade was about to close at quadrant I to IV (entering water surface) and open at quadrant III to II (leaving water surface). Blade opened to 45˚from its close position which parallel to rim. Wheel dimension was designed similarly with commonly used wheel size i.e. 20 cm width, 30 cm rim diameter and 60 cm total dimension.

Testing

Torque measurement is done using a strain gauge mounted on the wheel shaft. The sensor is connected to the strain amplifier (DAS–406B Strain Amp DC) through the slip ring and the bridge box recorded with the data logger (minilab 1008) and stored on the computer just as shown in Figure 1. Data measurement results in the form of voltage (mVolt) is converted into value strain (μst) and torque measurement values (N·m) to the value of the calibration has been done previously.

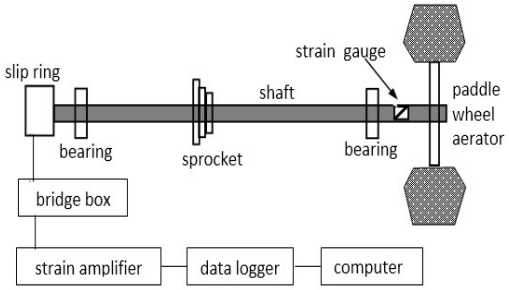

Figure1.Toque instrumen scheme

The measurement of paddlewheel power is done by measuring the power consumption of electric motors using Ammeter (DO2A) which is connected to an electrical output. To read the power measurement values (Watt) is done using a digital camera video recording on the screen Ammeter. Rated power is taken on an average value which often arises from the reading showing on video recordings.

Results and Discussion

Structural Design

The wheel structure consisted of two main components i.e.stationary and rotary component as shown in Figure 2.

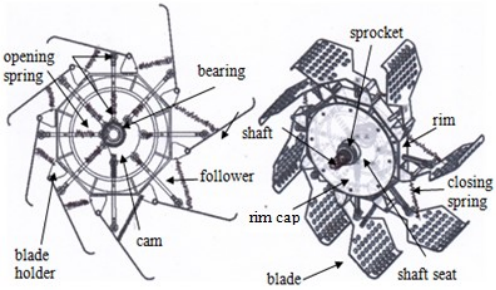

Figure2.Wheel structure with movable blade

Stationary component consisted of cam and shaft. The longest and shortest radius of cam were 680 mm and 17.5 mm, respectively. Cam was mounted to shaft with diameter of 25 mm and attached to machine frame.

Rotary component consisted of the rim, rim cap, blade holder, follower, bearing and spring. The rim was octagonal–shape encircling tube with diameter of 218 mm and height of 30 mm. One side of the tube was enclosed with metal sheet, shaft seat and bearing with diameter of 25 mm. Outside the shaft seat, sprocket that engage onto chain was attached for transmission purpose. The rim cap was a shaft seat made from metal sheet and similar bearing with rim tube which mounted to rim tube using bolt. Blade was used to directly splashing up water. Blades formed 30^0 of angle towards rim with radius of curvature was 40 cm. The

size of the blade was 15 cm of width, 20 cm of length, trapezoid–shape with 15^0 of bottom side and 30^0 of top side, had 40 holes with diameter of 1.6 cm. Blade holder was used to place blade with shaft of 8 mm and height of 25 mm and bolted at the end side of rim. The follower stem was used to push blade to open and close adjusting to cam profile. The follower stem was 150 mm of height and bearing with 19 mm of external diameter was attached on the two end–sides. Spring consisted of opening blade and closing blade. The opening spring was inserted to follower stem with diameter of the spring was 10.5 mm, length was 60 mm, wire diameter was 1 mm and spring constanta was 0.35 Nm. The closing spring of blade was attached on the front blade holder with diameter of 10 mm, length of 45 mm, wire diameter of 1 mm and spring constanta of 0.5 N·m.

Movable Components Mechanism

Movable blade were driven using cam mechanism. The cam is a simply mechanism that can provide almost all types of follower movement (Martin 1982). The movement analysis of cam mechanism is shown in Figure 3.

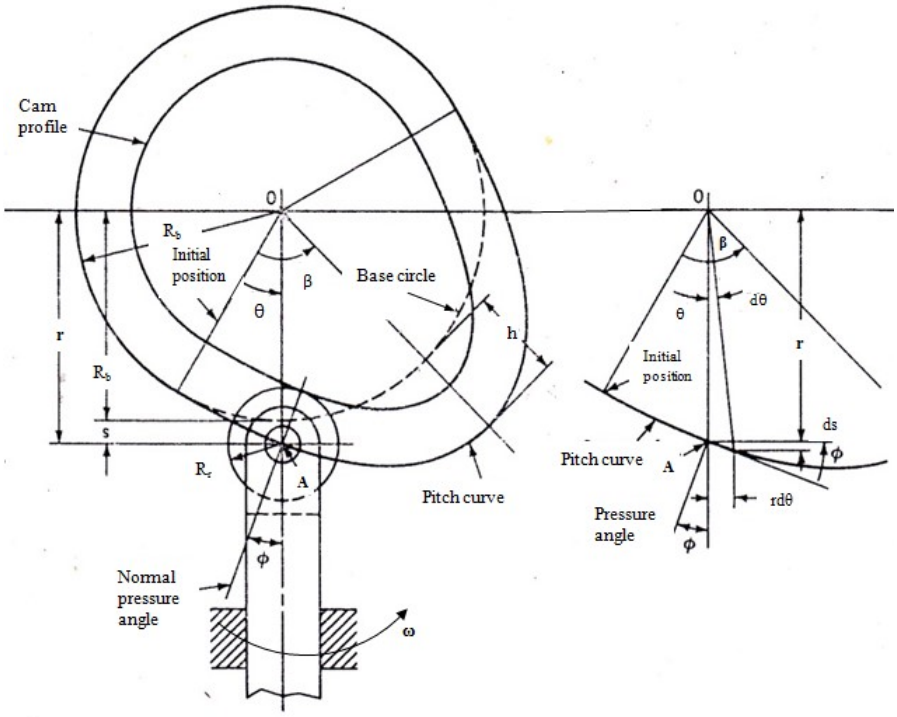

Figure. 3. Profile analysis of cam–follower

$$\text{for} \quad \frac{\theta}{\beta} \le 0.5 \qquad s = 2h\frac{\theta^2}{\beta^2}$$

$$\text{for} \quad \frac{\theta}{\beta} \ge 0.5 \qquad s = h\left[1-2\left(1-\frac{\theta}{\beta}\right)^2\right] \tag{1}$$

Equation of cam velocity is written as follows:

$$\text{for} \quad \frac{\theta}{\beta} \le 0.5 \qquad \frac{ds}{dt} = \frac{4h\omega\theta}{\beta^2}$$

$$\text{for} \quad \frac{\theta}{\beta} \ge 0.5 \qquad \frac{ds}{dt} = \frac{4h\omega}{\beta}\left(1-\frac{\theta}{\beta}\right) \tag{2}$$

Equation of cam acceleration is written as follows:

$$\text{for} \quad \frac{\theta}{\beta} \le 0.5 \qquad \frac{d^2s}{dt^2} = \frac{4h\omega^2}{\beta^2}$$

$$\text{for} \quad \frac{\theta}{\beta} \ge 0.5 \qquad \frac{d^2s}{dt^2} = -\frac{4h\omega^2}{\beta^2} \tag{3}$$

The result of follower displacement, velocity and acceleration is shown in Table 1.

Table 1. Normal force of cam–follower

θ (deg)	2πθ/β (deg)	t (s)	s (mm)	ds/dt (m/s)	d^2s/dt^2 (m^2/s)
0	0	0.00	0	0.00	6.09
12.5	36	0.05	1	0.11	6.09
25	72	0.10	4	0.22	6.09
37.5	108	0.16	9	0.33	6.09
50	144	0.21	16	0.44	6.09
62.5	180	0.26	25	0.55	6.09
62.5	180	0.26	25	0.55	-6.09
75	216	0.31	34	0.44	-6.09
87.5	252	0.37	41	0.33	-6.09
100	288	0.42	46	0.22	-6.09
112.5	324	0.47	49	0.11	-6.09
125	360	0.52	50	0.00	-6.09

The maximum displacement of follower for one rotation 50 mm with angle of rotation 125˚. The maximum velocity of follower was 0.55 m/s. The constant acceleration was 6.09 m/s^2.Angle of pressure determines the smoothness of cam movement. The analysis of angle of pressure was illustrated in Figure 3. Angle of pressure (Ø) for every angular position was equated as follows:

$$r = R_b + s$$
$$\tan \emptyset = \frac{ds}{r\, d\theta} \quad (4)$$

The magnitude of pressure angle for every angle of rotation is shown in Table 2.

Table 2. Normal force of cam follower

θ (deg)	2πθ/β (deg)	Ø (deg)	N (N)	Nx (N)	Ny (N)
0	0	0	239.64	239.64	0
12.5	36	18.13	-380.96	-362.05	-118.54
25	72	30.60	-146.87	-126.41	-74.77
37.5	108	37.38	-120.09	-95.43	-72.91
50	144	40.46	-122.97	-93.57	-79.79
62.5	180	41.40	-144.87	-108.68	-95.80
62.5	180	41.40	-144.87	-108.68	-95.80
75	216	31.01	-324.70	-278.29	-167.29
87.5	252	22.02	-3141.54	-2912.37	-1177.88
100	288	14.10	612.74	594.28	149.26
112.5	324	6.88	328.35	325.99	39.32
125	360	0	239.64	239.64	0

The largest angle of pressure between cam and follower was 41.40˚. This magnitude was too large and not necessary for cam–follower mechanism as it required high force and caused mechanism failure that led to machine damage.

Each blade had two types of spring i.e. blade–closing spring and blade–opening spring. Blade–closing spring (s_1) worked against drag force (F_d) and gravifty of the blade (w), while blade–opening spring (s_2) worked against force of blade–closing spring from cam pressure due to wheel rotation. Analysis of spring force is shown in Figure 4.

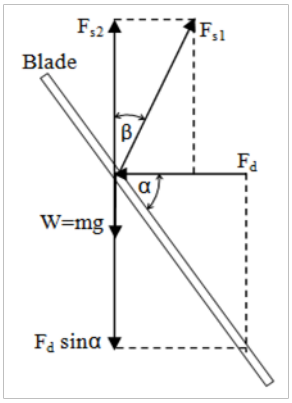

Figure 4. Spring force analysis

Based on the calculation, some of spring data were collected, including installed length, operating length, operating force, springs material, wire diameter, average diameter, inside diameter, outside diameter, free length, number of coils and allowable shear stress for blade–opening springs. The magnitude was 75 mm, 25 mm, 2.45 N, 49.05 N, chromium–vanadium A231, 2 mm, 2 mm, 10.5 mm, 14.5 mm, 80 mm, 12 coils and 922.74 MPa, respectively. The magnitude for blade–closing spring was 124 mm, 38 mm, 2.45 N, 264.50 N, chromium–vanadium A231, 2 mm, 2 mm, 8 mm, 125 mm, 130 mm, 20 coils and 815.75 MPa, respectively.

Innertia and torque analysis are shown in Figure 5. The influencing parameters consisted of force acting on follower (P), inertia force of follower (f), force of gravity on follower (W), shear stress acting on follower (F), normal force on rim towards follower (F_1, F_2), normal force of cam toward follower (N), follower overhang (a), distance between bearing surface (b), diameter of follower stem (d), pressure angle (Ø) and friction coefficient between follower (μ).

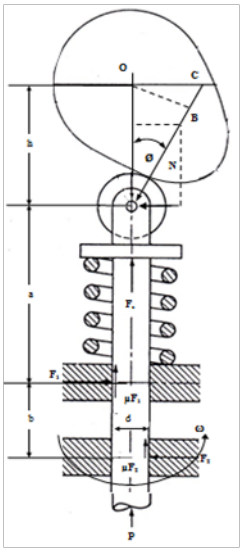

Figure 5. Analysis of angle of pressure

Total force along follower axis was:

$$F = P + f + W + F_s \quad (5)$$

Total vertical force was:

$$N \cos \emptyset = F + \mu (F_1 + F_2) \quad (6)$$

Total horizontal force was:

$$F_1 = F_2 + N \sin \emptyset \quad (7)$$

Summing moments to a point where F_1works, gave:

$$F_2(b - \mu d) = N_a \sin \emptyset + \frac{d}{2}(F - N \cos \emptyset) \quad (8)$$

By neglecting F_1 and F_2at the last 3 equations, normal force of cam acting on follower was:

$$N = \frac{F_b}{b\cos\emptyset - (2\mu a + \mu b - \mu^2 d)\sin\emptyset} \quad (9)$$

Torque required to rotate paddle wheel was calculated as follow:

$$T = N\,(OB) \quad (10)$$

The maximum torque required to activate blade mechanism was 80.09 N·m. Based on the required torque, using equation (6) and neglecting other mechanical loss, as much as 0.96 kW was required to rotate movable blade on paddle wheel aerator.

Torque and Power Consumption

Testing without a load at 115 rpm showed the torque that occured 43.05 N·m and the electric power used 511.72 Watt. Torque occuring reduction compared with calculation results due to modification follower. Follower rod are to be bent to minimize the contact angle that happened. That torque still high and not proportional to torque reduction of simulation result effect of using moveable blade 31.51% (Bahri *et al*. 2015). Thus, the electric power consumption was still high compared with Taiwan model paddlewheel aerator was 451 Watt. However, the resultsshowedthat the friction forcestill high occured between the cam and the follower that are caused by a cam profile which must follow the functional design of the padllewheel aerator.

Conclusion

Structure of the wheel consisted of two main components i.e. stationary and rotary component. Stationary component consisted of cam and shaft. Rotary component consisted of a rim, a rim cap, blade holders, followers, bearings and springs. The follower was able to rotate with angle of rotation was 125˚, rotational displacement was 50 mm, maximum velocity was 0.55 m/s and acceleration was 6.09 m/s^2. The follower had constant acceleration. Testing without a load at 115 rpm shows the torque that occured 43.05 N·m and the electric power used 511.72 Watt. These test results showed the friction forcestill high occured between the cam and the follower that are caused by a cam profile which must follow the functional design of the padllewheel aerator. It is suggested that to overcome the friction by increasing the dimension of mechanism contruction and reduce the angle contact between cam and follower.

References

Bahri, S., Setiawan, R. P. A., Hermawan, W. and Junior, M. Z.(2015). Design and simulation of paddle wheel aerator with movable blades. *International Journal of Engineering Research and Technology*. 4 (2):994–999.

Bhuyar, L. B., Thakre, S. B. and Ingole, N.W. (2009). Design characteristics of curved blade aerator w.r.t. aeration efficiency and overall oxygen transfer coefficient and comparison with CFDmodeling. *International Journal of Engineering,Science and Technology,* 1: 1–15.2009.

Boyd, C. E. (1988). Pond water aeration systems. *Aquaculture Engineering*, 18:9–40.1998.

Laksitanonta, S., Singh, S. and Singh, G.A.(2003). A review of aerators and aeration practices in Thai Aquaculture. *Agricultural Machanization in Asia, Africa and Latin America*, 34 (4):64–71.

Martin, G. H. (1982). *Kinematics and dynamics of machines*, USA:McGraw–Hill,Ltd. 194–382, 1982.

Moore, J. M. and Boyd, C.E. (1992). Design of small paddle wheel aerators. *Aquaculture Engineering,* 11:55–69.

Moulick, S., Mal, B. C. and Bandyopadhyay. (2002). Prediction of aeration performance of paddlewheel aerators. *Aquaculture Engineering,* 25:217–237.

Peterson, E. L. and Walker, M. B. (2002). Effect of speed on Taiwanese paddelwheel aeration. *Aquaculture Engineering*, 26:129–147.

Wyban, J. A., Pruder, G. D. and Leber, K.M. (1989). Paddle wheel effect on shrimp growth, production and crop value in commercial earthen ponds.*Journal of the World Aquaculture Society*, 20:18–23.